Current Research in Neurobiology 2 (2021) 100008

Contents lists available at ScienceDirect

Current Research in Neurobiology

journal homepage: www.editorialmanager.com/crneur/Default.aspx

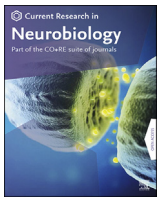

Evolution of interictal spiking during the latent period in a mouse model of mesial temporal lobe epilepsy

Maxime Lévesque [a], Anežka D.B. Macey-Dare [a], Siyan Wang [a], Massimo Avoli [a,b,*]

[a] Montreal Neurological Institute-Hospital & Department of Neurology & Neurosurgery; McGill University, Montréal, Québec, Canada
[b] Department of Physiology, McGill University, Montréal, Québec, Canada

ARTICLE INFO

Keywords:
Mesial temporal lobe epilepsy
Epileptogenesis
Interictal spikes
High-frequency oscillations
Latent period
Pilocarpine

ABSTRACT

Interictal spikes and high-frequency oscillations (HFOs, ripples: 80–200 Hz, fast ripples: 250–500 Hz) occur in epileptic patients and in animal models of mesial temporal lobe epilepsy (MTLE). In this study, we explored how type 1 and type 2 interictal spikes as well as ripples and fast ripples evolve during the latent period in the hippocampus of pilocarpine-treated mice. Depth EEG recordings were obtained from the hippocampus CA3 subfield of adult male mice (n = 5, P60–P100) starting one day before pilocarpine-induced status epilepticus up to the first spontaneous seizure, the so-called latent period. We found that rates of type 1 (n = 1 655) and type 2 (n = 2 309) interictal spikes were significantly lower during the late phase of the latent period compared to its early and mid phase ($p < 0.001$). However, rates of type 1 spikes associated with ripples (n = 266) or fast ripples (n = 106), as well as rates of type 2 interictal spikes associated with ripples (n = 233), were significantly higher during the late phase compared to the early and mid phases ($p < 0.05$). Our findings reveal that an increase of type 1 interictal spikes co-occurring with ripples or fast ripples and an increase of type 2 interictal spikes co-occurring with ripples mark the end of the latent period. We propose that changes in the occurrence of interictal spike associated with HFOs represent a biomarker of epileptogenicity in this mouse model of MTLE.

1. Introduction

Mesial temporal lobe epilepsy (MTLE) is the most common form of focal epilepsy with seizures originating from the hippocampus, amygdala or entorhinal cortex (EC) (Engel, 1996; Spencer and Spencer, 1994). These focal seizures emerge after a seizure-free latent period of several years following an initial brain insult such as status epilepticus (SE), traumatic brain injury, or encephalitis (Banerjee et al., 2009; De Lanerolle et al., 2003; Engel, 1996; French et al., 1993; Gloor, 1997; Salanova et al., 1994; Wieser, 2004). Therapeutic approaches, once seizures appear, are often limited to symptomatic management with low success rates since nearly one-third of cases are resistant to anti-epileptic drugs, which leaves a large proportion of patients with intractable MTLE (Engel et al., 2012). Chronic seizures cause cognitive decline (wen Xu et al., 2018; Zemlyanaya et al., 2018), secondary mental health illnesses and increased mortality (Gilliam et al., 2003; Kessler et al., 2012; Laxer et al., 2014), thus presenting a significant burden for both patients and wider society.

There is strong evidence suggesting that the latent period houses *epileptogenesis*, an insult-induced cascade of cellular and molecular alterations that lead to subsequent reorganisation of neuronal networks, transforming the brain from healthy to epileptic (Dudek and Staley, 2013; Löscher and Brandt, 2010; Pitkänen and Lukasiuk, 2011). These data have been obtained in animals, especially rodents, in which the duration of the latent period is shorter than what is observed in humans. In these animal models of MTLE, biomarkers such as interictal spikes associated with high-frequency oscillations (HFOs, ripples: 80–200 Hz, fast ripples: 250–500 Hz) have been discovered and they have been associated with epileptogenesis since, following the initial SE, they precede the appearance of spontaneous recurrent seizures (i.e., the chronic epileptic condition) (Jefferys et al., 2012). Different types of interictal spikes (type 1 and type 2), based on their morphological features, have also been identified in rats in the kainic acid and pilocarpine models of MTLE. Specifically, it was found that the frequency of type 1 interictal spikes (a spike followed by a long-lasting wave) decreases shortly before the occurrence of the first seizure whereas rates of type 2 interictal spikes (a spike with no wave) increase (Chauvière et al., 2012); moreover, a successive study has revealed that type 2 interictal spikes associated with fast ripples predominate during the last two days of the latent period in the EC compared to the CA3 region of the hippocampus, whereas both

* Corresponding author. Montreal Neurological Institute, 3801 University Street, Montréal, QC, H3A 2B4, Canada.
E-mail address: massimo.avoli@mcgill.ca (M. Avoli).

https://doi.org/10.1016/j.crneur.2021.100008
Received 26 November 2020; Received in revised form 26 February 2021; Accepted 2 March 2021

types occur at similar rate in CA3 and EC during the following chronic epileptic period (Salami et al., 2014).

It is unclear whether type 1 and type 2 interictal spikes are also present in mouse models of MTLE, and whether patterns of occurrence similar to those identified in rats are observed. Mice, compared to rats, are highly sensitive to pilocarpine (Curia et al., 2008), and show immediate neurotoxic and inflammatory effects that could favor neuronal hyperexcitability (Pitsch et al., 2017) and "rapid" epileptogenesis (Mazzuferi et al., 2012; Wang et al., 2019). Therefore, in this study, we analysed the temporal evolution of type 1 and type 2 interictal spikes as well as of ripples (80–200 Hz) and fast ripples (250–500 Hz) in the hippocampus of pilocarpine-treated mice, from the end of SE to the onset of the first spontaneous seizure.

2. Methods

Animals – Adult male mice (n = 5, P60–P100) were maintained in controlled conditions (22 ± 2 °C, 12-h light/dark cycle) with food and water *ad libitum*. The sample consisted of four Pv-ChR2 mice and one Pv-Cre mouse. PV-ChR2 animals were obtained from cross-breeding PV-Cre [B6;129P2-*pvalb*$^{tm1(cre)Arbr}$/J, The Jackson Laboratory; RRID: IMSR_JAX:008069] with Ai32 mice [R26-lox-stop-lox-ChR2(H134R)-EYFP, The Jackson Laboratory; RRID IMSR_JAX:012569]. All animals were bred and maintained in-house. We could not find any differences between strains regarding their sensitivity to pilocarpine; all animals exhibited a similar response to the chemoconvulsant. Procedures were performed according to the guidelines of the Canadian Council on Animal Care and approved by the Animal Care Committee of McGill University.

Stereotaxic surgery – A schematic diagram of the protocol is shown in Fig. 1A. Mice were anaesthetized with 3% isoflurane in 100% O_2 and fixed in a stereotaxic frame. An incision was made in the skin and one anchor screw (2.4 mm length) was fixed to the skull. One small hole was drilled over the left CA3 subfield of the hippocampus (AP: - 2.85, ML: 3, DV: - 4) to allow the implantation of a bipolar electrode (20–30 kΩ). A second hole was drilled in the frontal bone to allow the implantation of the reference (5–10 kΩ), which consisted of an electrode from which insulation was removed and that was bent at 90° angle to overlie the cortex. The screw, electrode, fibers and reference were covered with dental cement. After surgery, mice received topic application of chloramphenicol (Erfa, Qc, Canada) and lidocaine (5%; Odan, Qc, Canada) and were injected with carprofen every 24 h (20 mg/kg s.c.; Merail, Qc, Canada), buprenorphine every 8 h (0.1 mg/kg s.c., CDMV, Qc, Canada), enrofloxacin every 24 h (5 mg/kg, s.c., CDMV, Qc, Canada) and 1 ml of 0.9% saline every 24 h (s.c.) for 72 h post-op.

Video-EEG recordings - Mice were housed in custom-designed Plexiglas boxes. After a 7-day recovery period, electrodes were connected to a multichannel cable (HRS Scientific, Canada). Continuous video-EEG recordings were started one day before the induction of SE and continued until the first spontaneous seizure. EEG signals were amplified with a mobile 36ch interface tool (Stellate, Canada) and high-pass filtered at 0.1 Hz (2nd order infinite impulse response filter) with a sampling rate of 2000 Hz per channel. A 500 Hz low-pass hardware filter was used to minimize aliasing. Monitoring software (Harmonie, Stellate, Canada) was used to integrate time-stamped video files with EEG data.

Induction of status epilepticus – One week after electrode implantation, mice were injected with scopolamine methylnitrate (1 mg/kg, i.p.), followed 30 min later by up to 6 injections of pilocarpine (50–100 mg/kg at 30 min intervals) until the occurrence of SE, which was defined as convulsive seizure activity lasting for more than 5 min

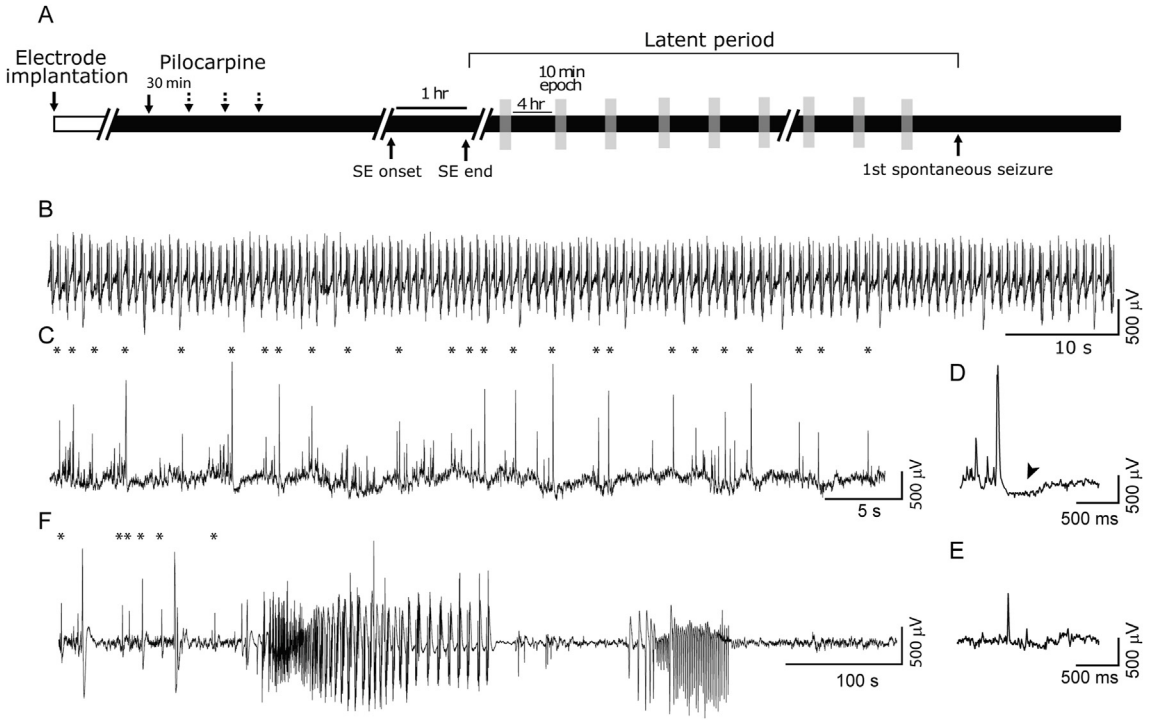

Fig. 1. – A: Schematic diagram of the experimental protocol. One week after electrode implantation, mice were injected with scopolamine methylnitrate (1 mg/kg, i.p.), followed 30 min later by up to 6 injections of pilocarpine (50–100 mg/kg at 30 min intervals) until the occurrence of SE, which was terminated after 1 h with diazepam and ketamine. The latent period was defined as the period between the end of SE and the occurrence of the first spontaneous seizure. Epochs of 10 min of EEG recordings were extracted every 4 h during the latent period. **B**: EEG recordings showing SE activity in one animal. **C**: Interictal activity in the same animal as in **B**, one day after SE. Interictal spikes that were detected by the algorithm are indicated with asterisks (*); artefacts were removed after visual inspection of EEG traces. **D**: Representative example of a type 1 interictal spike from another pilocarpine-treated animal. Note the presence of a wave after the peak (arrowhead). **E**: Representative example of a type 2 interictal spike from a third pilocarpine-treated animal. **F**: First spontaneous seizure in the same animal as shown in B and C. Interictal spikes that were detected by the algorithm are indicated with asterisks (*); artefacts were removed after visual inspection of EEG traces.

(Fig. 1B). SE was terminated after 1 h by injecting diazepam (10 mg/kg, s.c.; CDMV, Qc, Canada) and ketamine (25 mg/kg, s.c.; CDMV, Qc, Canada) (Lévesque et al., 2019).

Interictal spikes and HFO analysis – EEG recordings were sampled as 10-min epochs every 4 h with the first epoch extracted immediately after SE termination and the final epoch extracted at least 1 h prior to the onset of the first spontaneous seizure (Fig. 1A). Epochs were only selected when mice were sleeping or immobile to minimize movement artefacts and maximise HFO detection (Bagshaw et al., 2009; Staba et al., 2004). They were then exported to MATLAB 2019b (MathWorks, USA) and artefacts removed by visual inspection. Epochs were analysed for interictal spikes and HFOs (minimum order equiripple bandpass filters; ripples: 80–200 Hz, fast-ripples: 250–500 Hz) with custom-designed algorithms using methods previously published (Lévesque et al., 2019) and outlined below.

The end of SE was defined as termination of continuous spiking activity and return to baseline EEG activity (Wang et al., 2019). The latent period was defined as the time between the end of SE and the onset of the first spontaneous seizure (Fig. 1A). The duration of the latent period was converted into a 0–100% scale, with 0% representing the end of SE and 100% the onset of the first spontaneous seizure. Counts of interictal spikes and HFOs were calculated in 1% bins and averaged across mice, to allow comparison of rates over variable time lengths. To exclude any effects due to variability in interictal spike occurrence, the ratio of interictal spikes with HFOs to interictal spikes was calculated per 1% bin.

Interictal spikes were defined as isolated irregular spikes having an amplitude ≥5 SD above the baseline mean (Wang et al., 2019) (Fig. 1C). They were subsequently classified into type 1 (interictal spike with a wave) (Fig. 1D) and type 2 (interictal spike with no wave) (Fig. 1E), as previously defined (Chauvière et al., 2012; Salami et al., 2014). HFOs were defined as events with four consecutive oscillatory cycles with amplitude >3 SD above the baseline mean, in the 80–200Hz (ripples) and 250–500Hz (fast ripples) frequency bands (Lévesque et al., 2019). Overlapping HFOs were excluded from analysis (Bénar et al., 2010). HFOs were defined as co-occurring with an interictal spike if they occurred within 500 ms of the peak of the interictal spike. The occurrence of the first spontaneous seizure (Fig. 1F) marked the end of the latent period.

Statistical analyses - All statistical analyses were performed in MATLAB 2019b (MathWorks, USA). To compare changes within rates of interictal spikes and HFOs, data samples from the early (0–20%), mid (40–60%) and late (80–100%) phase of the latent period were averaged together in each category and plotted as mean ± SEM, then compared. Normality was assessed using the Shapiro-Wilks test. For parametric data, we performed repeated measures ANOVAs followed by post-hoc Student's t-tests with Bonferroni corrections. Likewise, for non parametric data, we performed Friedman tests followed by post-hoc Wilcoxon Rank Sum tests with Bonferroni corrections. The level of significance was set at $p < 0.05$ (*$p < 0.05$, **$p < 0.01$).

3. Results

Interictal spikes - All animals (n = 5) showed spontaneous seizures, on average 5.1 (±3.0) days after SE. Fig. 2A shows average rates of the total number of interictal spikes (n = 4 053) over time during the latent period, on a 0–100% scale. When comparing the early (0–20%), mid (40–60%) and late (80–100%) phases of the latent period, we found significant differences that indicated a decrease in the total number of interictal spikes over time (Friedman test: $X^2r = 33.4$, $p < 0.0001$, Post-hoc Wilcoxon Rank Sum tests with Bonferroni corrections: early vs mid: $p = 0.186$; mid vs late: **$p < 0.01$; early vs late: **$p < 0.01$) (Fig. 2B).

We next investigated type 1 and type 2 interictal spikes, to determine whether their occurrence changed during the latent period. Type 1 interictal spikes represented 40.8% (n = 1 655, average duration = 394.1 ± 6.4 ms) of the total number of interictal spikes. Overall, rates of type 1 interictal spike decreased over time (Fig. 2C), as revealed by the comparisons of the early, mid and late phases of the latent period (repeated measures ANOVA: $F(2, 40) = 78.9$, $p < 0.0001$, Student's t-tests with Bonferroni corrections: early vs mid: **$p < 0.01$; mid vs late: **$p < 0.01$; early vs late: **$p < 0.01$) (Fig. 2D). Similar results were

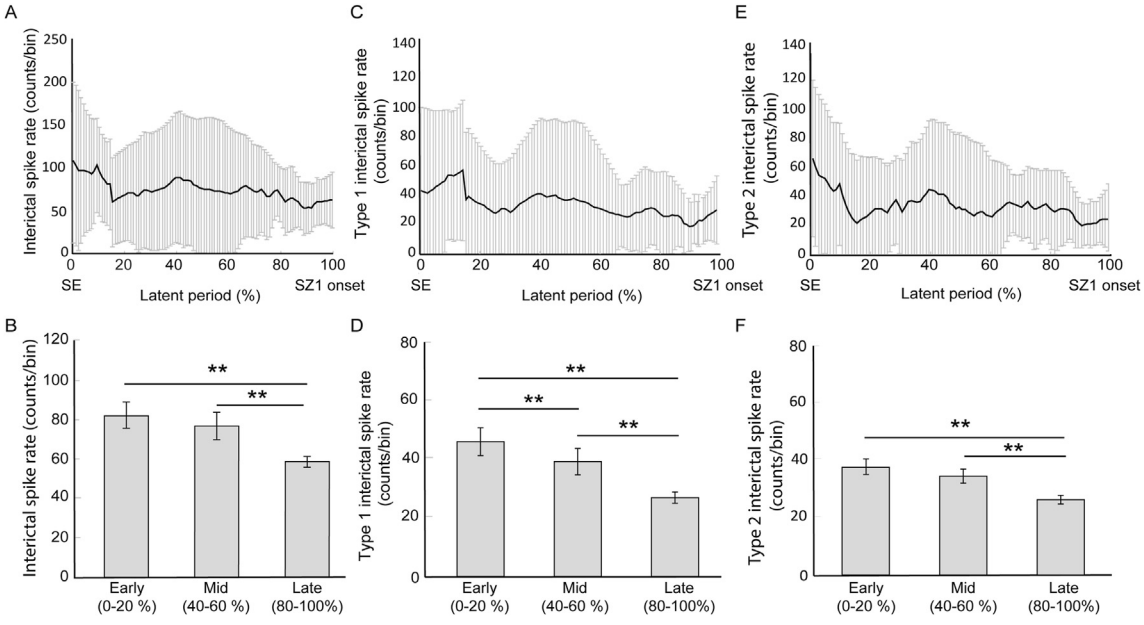

Fig. 2. - A: Rates of interictal spikes over time, from the end of SE to the onset of the latent period or the occurrence of the first spontaneous seizure (SZ1 onset). The latent period is converted into a scale from 0 (end of SE) to 100% (time of the first seizure occurrence) to account for differences in duration between animals (mean ± SD). **B:** Bar graph showing the average rates of interictal spikes for the early (0–20%), mid (40–60%) and late (80–100%) phase of the latent period. Note that interictal spike rates significantly decreased over time. **C:** Rates of type 1 interictal spikes over time during the latent period. **D:** Bar graph showing average rates of type 1 interictal spikes during the early, mid and late phase of the latent period. Rates of type 1 interictal spikes significantly decreased over time. **E:** Rates of type 2 interictal spikes over time during the latent period. **F:** Bar graph showing average rates of type 2 interictal spikes during the early, mid and late phase of the latent period. Type 2 interictal spike rates also decreased significantly over time before the first spontaneous seizure. **$p < 0.01$.

observed for type 2 interictal spikes, which represented 56.9% (n = 2 309, average duration = 215.7 ± 5.9 ms) of the total number of interictal spikes. They significantly decreased over time (Fig. 2E), as shown by comparing their rates of occurrence during the three phases of the latent period (Friedman test: $X^2r = 32.6$, $p < 0.0001$, Post-hoc Wilcoxon Rank Sum tests with Bonferroni corrections: early vs mid: $p = 1.074$; mid vs late: $^{**}p < 0.01$; early vs late: $^{**}p < 0.01$) (Fig. 2F). A total of 89 interictal spikes (2.19%) could not be classified as either type 1 or type 2 and were excluded from further analysis.

Interictal spikes co-occurring with high-frequency oscillations – Next, we analysed interictal spikes co-occurring with ripples (n = 492) and found that they significantly increased in occurrence at the end of the latent period (Fig. 3A), before the onset of the first spontaneous seizure (repeated measures ANOVA: $F(2, 40) = 89.2$, $p < 0.0001$, Student's t-tests with Bonferroni corrections: early vs mid: $^{*}p < 0.05$; mid vs late: $^{**}p < 0.01$; early vs late: $^{**}p < 0.01$) (Fig. 3B). This pattern was observed for type 1 interictal spikes co-occurring with ripples (Fig. 3C) (n = 266) (repeated measures ANOVA: $F(2, 40) = 28.5$, $p < 0.0001$, Student's t-tests with Bonferroni corrections: early vs mid: $p = 0.156$; mid vs late: $^{**}p < 0.01$; early vs late: $^{**}p < 0.01$) (Fig. 3D and E) and for type 2 interictal spikes co-occurring with ripples (Fig. 3F) (n = 223) (Friedman test: $X^2r = 20.7$, $p < 0.0001$, Post-hoc Wilcoxon rank sum tests with Bonferroni corrections: early vs mid: $p = 1.074$; mid vs late: $^{**}p < 0.01$; early vs late: $^{*}p < 0.05$) (Fig. 3G and H). Therefore, both type 1 and type 2 interictal spikes co-occurring with ripples significantly increased at the end of the latent period, before the occurrence of the first spontaneous seizure.

Interictal spikes co-occurring with fast ripples (n = 188) also significantly increased in occurrence before the first spontaneous seizure (repeated measures ANOVA: $F(2, 40) = 36.1$, $p < 0.0001$, Student's t-tests with Bonferroni corrections: early vs mid: $^{*}p < 0.05$; mid vs late: $^{**}p < 0.01$; early vs late: $^{**}p < 0.01$) (Fig. 4A and B). Similar results were observed for type 1 interictal spikes with fast ripples (Fig. 4C) (n = 106) (repeated measures ANOVA: $F(2, 40) = 45.6$, $p < 0.0001$, Student's t-tests with Bonferroni corrections: early vs mid: $^{**}p < 0.01$; mid vs late: $^{**}p < 0.01$; early vs late: $^{**}p < 0.01$) (Fig. 4D and E). Type 2 interictal spikes with fast ripples (Fig. 4F) (n = 80), however, appeared to decrease over time, although this trend did not reach statistical significance (Friedman test: $X^2r = 3.5$, $p = 0.17$) (Fig. 4G and H).

Finally, we analysed isolated HFOs (n = 594) that occurred independently of interictal spikes. We found that isolated ripples (Fig. 5A) (n = 447) significantly increased in occurrence before the first spontaneous seizure (repeated measures ANOVA: $F(2, 40) = 56.3$, $p < 0.0001$, Student's t-tests with Bonferroni corrections: early vs mid: $^{**}p < 0.01$; mid vs late: $p = 2.4$; early vs late: $^{**}p < 0.01$) (Fig. 5B and C). Isolated fast ripples (Fig. 5D) were also observed (n = 147); however, they did not

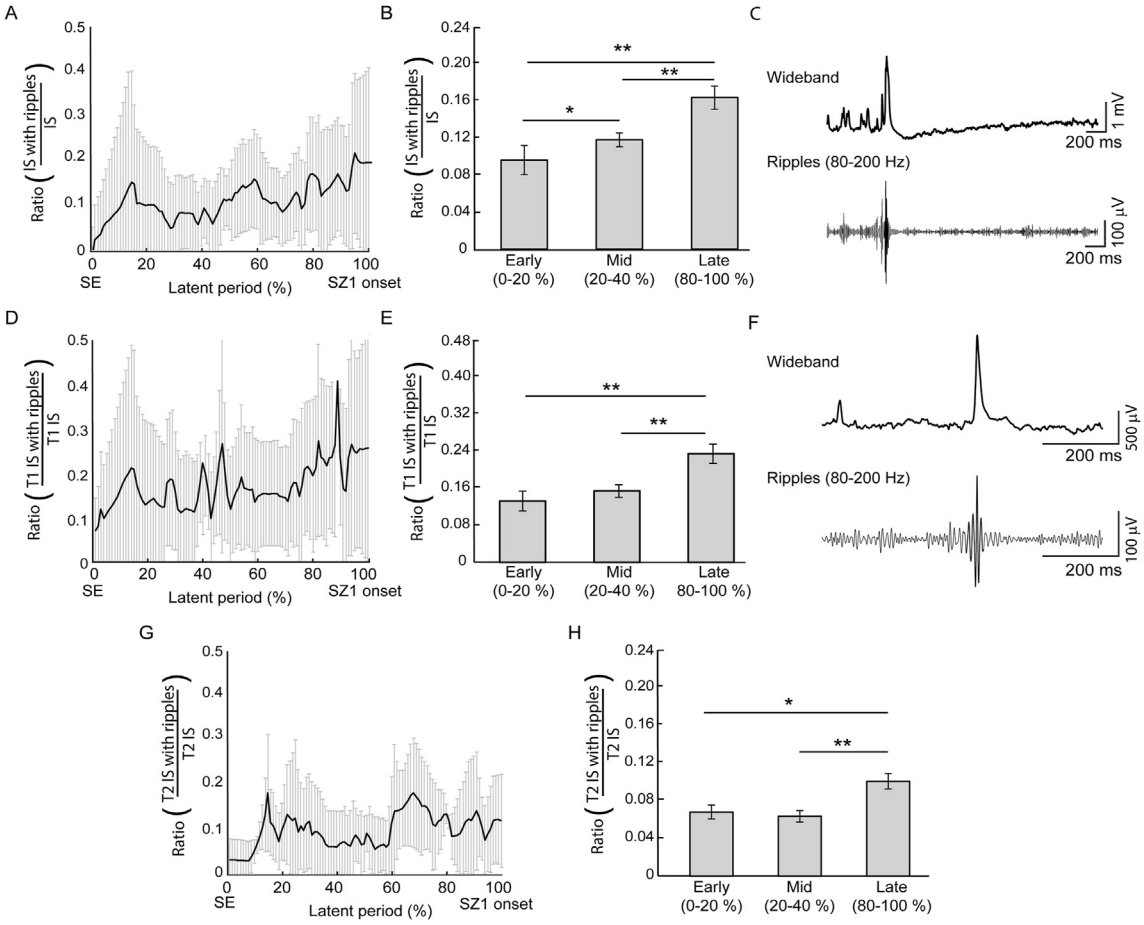

Fig. 3. – A: Ratios of interictal spikes co-occurring with ripples on the total number of interictal spikes over time during the latent period. **B:** Bar graph showing average ratios of interictal spikes with ripples during the early, mid and late phase of the latent period; a significant increase over time was observed. **C:** Representative example of type 1 interictal spike co-occurring with a ripple. **D**: Ratios of type 1 interictal spikes with ripples on the total number of type 1 interictal spikes during the latent period. **E:** Bar graph showing the average ratios of type 1 interictal spikes with ripples during the early, mid and late phase of the latent period. Note that type 1 interictal spikes with ripples significantly increased over time. **F**: Representative example of a type 2 interictal spike co-occurring with a ripple. **G:** Ratios of type 2 interictal spikes with ripples on the total number of type 2 interictal spikes during the latent period. **H:** Bar graph showing the average ratios of type 2 interictal spikes with ripples during the early, mid and late phase of the latent period; a significant increase was observed over time. $^{*}p < 0.05$, $^{**}p < 0.01$. IS = interictal spikes; T1 IS = type 1 interictal spikes, T2 IS = type 2 interictal spikes.

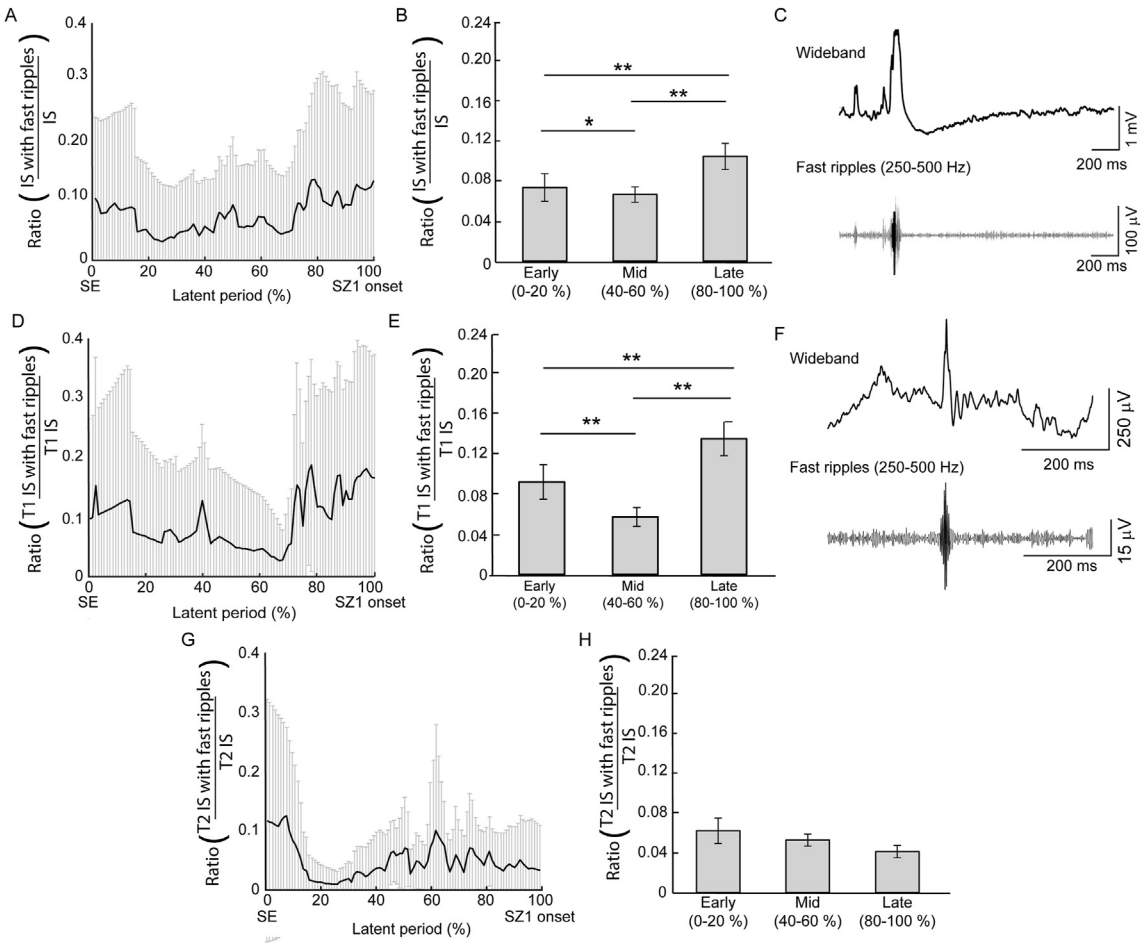

Fig. 4. – **A**: Ratios of the total number of interictal spikes with fast ripples on the total number of interictal spikes during the latent period. **B:** Bar graph showing the average ratios of interictal spikes with fast ripples during the early, mid and late phase of the latent period. A significant increase was observed at the end of the latent period. **C**: Representative example of a type 1 interictal spike co-occurring with a fast ripple. **D:** Ratios of type 1 interictal spikes with fast ripples on the total number of type 1 interictal spikes during the latent period. **E:** Bar graph showing the average ratios of type 1 interictal spikes with fast ripples during the early, mid and late phase of the latent period. A significant increase was observed at the end of the latent period. **F**: Representative example of a type 2 interictal spike co-occurring with a fast ripple. **G:** Ratios of type 2 interictal spikes with fast ripples on the total number of type 2 interictal spikes. **H**: Bar graph showing the average ratios of type 2 interictal spikes with fast ripples during the early, mid and late phase of the latent period. No significant difference was observed among the three phases. *$p < 0.05$, **$p < 0.01$. IS = interictal spikes; T1 IS = type 1 interictal spikes, T2 IS = type 2 interictal spikes.

show any significant change in rate during the latent period (Friedman test: $X^2r = 3.0$, $p = 0.22$) (Fig. 5E and F).

4. Discussion

The main findings of our study can be summarised as follows: (i) type 1 and type 2 interictal spikes significantly decrease in occurrence shortly before the first spontaneous seizure; (ii) rates of type 1 interictal spikes co-occurring with ripples or fast ripples significantly increase at the end of the latent period, along with the rates of type 2 interictal spikes co-occurring with ripples; (iii) rates of type 2 interictal spikes co-occurring with fast ripples do not change over time; and (iv) isolated ripples increase in occurrence before the first spontaneous seizure whereas no significant change is identified for fast ripples.

Interictal spikes with different durations and distinct morphological features were found during the chronic period in the hippocampus CA3 subfield and in the entorhinal cortex of epileptic rats treated with pilocarpine by Bortel et al. (2010) who, however, did not classified them as type 1 and type 2. Shortly later, Chauvière et al. (2012) classified interictal spikes based on their morphological features in pilocarpine- and kainic acid-treated rats and reported that they have different patterns of occurrence during the latent period. Specifically, they reported that type 1 interictal spikes (which are followed by long-lasting waves) gradually decrease in frequency during the latent period, whereas type 2 interictal spikes (which are not followed by long-lasting waves) significantly increase, reaching their minimum/maximum value before the first spontaneous seizure. An increase of occurrence of type 2 interictal spikes in the CA3 region of epileptic rats, before first seizure occurrence, was also reported by Salami et al. (2014) in the pilocarpine model.

Chauvière et al. (2012) proposed that type 1 interictal spikes correspond to the recruitment of large populations of excitatory and inhibitory cells whereas type 2 interictal spikes would reflect local activity of excitatory neurons. Changes in type 2 interictal spike frequency were therefore attributed to the progressive buildup of excitatory circuits during epileptogenesis (Chauvière et al., 2012). In contrast, in this study we have found in mice that the occurrence of both type 1 and type 2 interictal spikes decreases from the end of SE to the onset of the first spontaneous seizure. The discrepancy between our present results and those reported in previous studies (Chauvière et al., 2012; Salami et al., 2014) could be due to inter-species differences, since mice and rats show different levels of sensitivity to chemoconvulsants. Indeed, compared to rats, mice are highly sensitive to pilocarpine, which translates into high mortality rates in this species (Curia et al., 2008) as well as immediate neurotoxic and inflammatory effects, which could favor neuronal

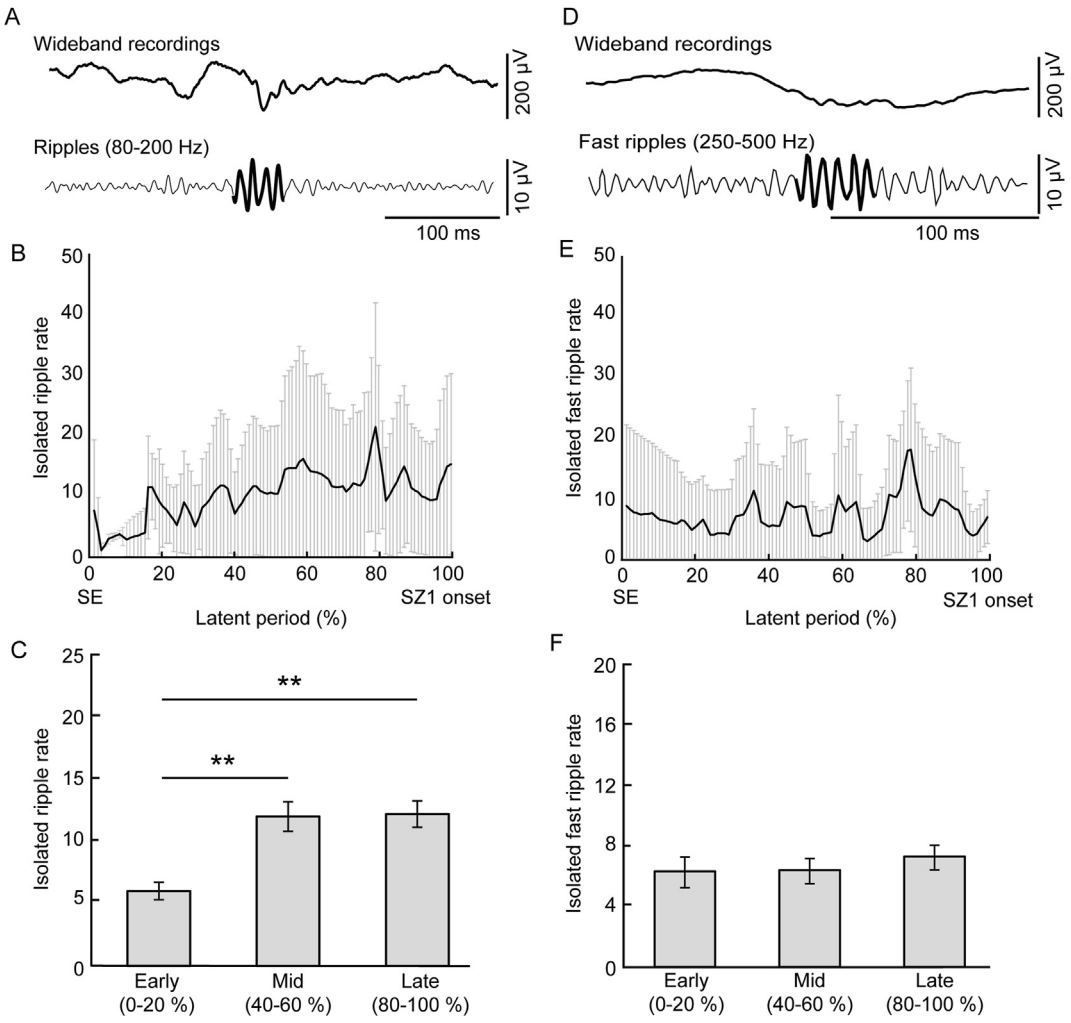

Fig. 5. **– A:** Representative example of an isolated ripple (80–200 Hz). **B:** Rates of isolated ripples over time during the latent period. **C:** Bar graph showing the average rate of isolated ripples during the early, mid and late phase of the latent period; a significant increase of isolated ripple rates was observed over time. **D:** Representative example of an isolated fast ripple (250–500 Hz). **E:** Rates of isolated fast ripples over time. **F:** Bar graph showing the average rate of isolated fast ripples during the early, mid and late phase of the latent period. No significant differences were observed. **$p < 0.01$.

hyperexcitability (Pitsch et al., 2017). In line with this hypothesis, the latent period in pilocarpine-treated mice is practically non-existent, since seizures can occur within the first 48 h after SE (Mazzuferi et al., 2012; Pitsch et al., 2017; Wang et al., 2019).

Our present data show that type 1 interictal spikes associated with ripples or fast ripples as well as type 2 interictal spikes associated with ripples significantly increase before the occurrence of the first spontaneous seizure. Ripples and fast ripples (i.e., HFOs) are considered as biomarkers of pathological network synchronization (Jefferys et al., 2012). HFOs both in the ripple and fast ripple frequency range were observed before the first spontaneous seizure in kainic acid- (Bragin et al., 2004) and pilocarpine-treated animals (Salami et al., 2014). No significant increase of type 2 interictal spikes associated with fast ripples was, however, observed before the occurrence of the first seizure; such increased instead occur in rats later during the chronic epileptic stage, as it was reported in the study of Salami et al. (2014), in which type 2 interictal spikes associated with fast ripples reached their maximum frequency 48h after the first seizure.

Finally, we have found that isolated ripples, but not isolated fast ripples, occurred at significantly higher rates during the mid and late phases of the latent period. Ripples, which presumably represent population IPSPs generated by principal neurons entrained by synchronously active interneuron networks (Buzsáki and Chrobak, 1995; Ylinen et al., 1995), could therefore reach their maximum value before the onset of spontaneous seizures. The presence of isolated fast ripples, thought to reflect the synchronous firing of principal (glutamatergic) neurons in the epileptic hippocampus of animals and patients (Bragin et al., 2011; Foffani et al., 2007; Ibarz et al., 2010) could however be more restricted to the chronic epileptic state.

5. Conclusions

Our findings reveal that interictal spikes and their associated HFOs display different patterns of evolution during the latent period in the mouse pilocarpine model of MTLE. An increase of type 1 interictal spikes associated with ripples and fast ripples as well as type 2 interictal spikes associated with ripples mark the end of the latent period. We propose that analyzing different types of interictal spikes may help to better understand the transition from a latent to a chronic epileptic state.

CRediT author statement

Maxime Lévesque: Conceptualization, Methodology, Formal analysis, Writing-Original Draft, Writing-Review & Editing, Visualization, Supervision, Project Administration. **Anežka D.B. Macey-Dare:** Methodology, Formal analysis, Writing-Original Draft, Writing-Review &

Editing, Visualization. **Siyan Wang:** Conceptualization, Methodology, Software, Formal analysis, Writing-Review & Editing, Software. **Massmimo Avoli:** Conceptualization, Methodology, Investigation, Writing-Original Draft, Writing-Review & Editing, Visualization, Supervision, Project Administration, Funding Acquisition.

Declaration of competing interest

The authors declare that they have no known competing financial interests or personal relationships that could have appeared to influence the work reported in this paper.

Acknowledgments

This study was supported by the Canadian Institutes of Health Research (PJT153310, PJT166178 and MOP130328) and the Savoy Foundation (M.A.). AMD was the recipient of the Imperial College Faculty of Medicine-McGill Exchange Scholarship.

Appendix A. Peer Review Overview and Supplementary data

A Peer Review Overview and (sometimes) Supplementary data associated with this article can be found, in the online version, at https://doi.org/10.1016/j.crneur.2021.100008.

References

Bagshaw, A.P., Jacobs, J., LeVan, P., Dubeau, F., Gotman, J., 2009. Effect of sleep stage on interictal high-frequency oscillations recorded from depth macroelectrodes in patients with focal epilepsy. Epilepsia 50, 617–628.
Banerjee, P.N., Filippi, D., Allen Hauser, W., 2009. The descriptive epidemiology of epilepsy-A review. Epilepsy Res. 85, 31–45.
Bénar, C.G., Chauvière, L., Bartolomei, F., Wendling, F., 2010. Pitfalls of high-pass filtering for detecting epileptic oscillations: a technical note on "false" ripples. Clin. Neurophysiol. 121, 301–310.
Bortel, A., Lévesque, M., Biagini, G., Gotman, J., Avoli, M., 2010. Convulsive status epilepticus duration as determinant for epileptogenesis and interictal discharge generation in the rat limbic system. Neurobiol. Dis. 40, 478–489.
Bragin, A., Benassi, S.K., Kheiri, F., Engel Jr., J., 2011. Further evidence that pathologic high-frequency oscillations are bursts of population spikes derived from recordings of identified cells in dentate gyrus. Epilepsia 52, 45–52.
Bragin, A., Wilson, C.L., Almajano, J., Mody, I., Engel, J., 2004. High-frequency oscillations after status epilepticus: epileptogenesis and seizure genesis. Epilepsia 45, 1017–1023.
Buzsáki, G., Chrobak, J.J., 1995. Temporal structure in spatially organized neuronal ensembles: a role for interneuronal networks. Curr. Opin. Neurobiol. 5, 504–510.
Chauvière, L., Doublet, T., Ghestem, A., Siyoucef, S.S., Wendling, F., Huys, R., Jirsa, V., Bartolomei, F., Bernard, C., 2012. Changes in interictal spike features precede the onset of temporal lobe epilepsy. Ann. Neurol. 71, 805–814.
Curia, G., Longo, D., Biagini, G., Jones, R.S.G., Avoli, M., 2008. The pilocarpine model of temporal lobe epilepsy. J. Neurosci. Methods 172, 143–157.
De Lanerolle, N.C., Kim, J.H., Williamson, A., Spencer, S.S., Zaveri, H.P., Eid, T., Spencer, D.D., 2003. A retrospective analysis of hippocampal pathology in human temporal lobe epilepsy: evidence for distinctive patient subcategories. Epilepsia 44, 677–687.
Dudek, F.E., Staley, K.J., 2013. The time course and circuit mechanisms of acquired epileptogenesis. In: Jaspers Basic Mech. Epilepsies. Oxford University Press, pp. 405–415.
Engel, J., 1996. Introduction to temporal lobe epilepsy. Epilepsy Res. 26, 141–150.
Engel, J., McDermott, M.P., Wiebe, S., Langfitt, J.T., Stern, J.M., Dewar, S., Sperling, M.R., Gardiner, I., Erba, G., Fried, I., Jacobs, M., Vinters, H.V., Mintzer, S., Kieburtz, K., 2012. Early surgical therapy for drug-resistant temporal lobe epilepsy. J. Am. Med. Assoc. 307, 922–930.
Foffani, G., Uzcategui, Y.G., Gal, B., Menendez de la Prida, L., 2007. Reduced spike-timing reliability correlates with the emergence of fast ripples in the rat epileptic Hippocampus. Neuron 55, 930–941.
French, J.A., Williamson, P.D., Thadani, V.M., Darcey, T.M., Mattson, R.H., Spencer, S.S., Spencer, D.D., 1993. Characteristics of medial temporal lobe epilepsy: I. Results of history and physical examination. Ann. Neurol. 34, 774–780.
Gilliam, F., Hecimovic, H., Sheline, Y., 2003. Psychiatric comorbidity, health, and function in epilepsy. Epilepsy Behav. 4.
Gloor, Pierre, 1997. The Temporal Lobe and Limbic System. Oxford University Press.
Ibarz, J.M., Foffani, G., Cid, E., Inostroza, M., de la Prida, L.M., 2010. Emergent dynamics of fast ripples in the epileptic Hippocampus. J. Neurosci. 30, 16249–16261.
Jefferys, J.G.R., Menendez de la Prida, L., Wendling, F., Bragin, A., Avoli, M., Timofeev, I., Lopes da Silva, F.H., 2012. Mechanisms of physiological and epileptic HFO generation. Prog. Neurobiol. 98, 250–264.
Kessler, R.C., Lane, M.C., Shahly, V., Stang, P.E., 2012. Accounting for comorbidity in assessing the burden of epilepsy among US adults: results from the National Comorbidity Survey Replication (NCS-R). Mol. Psychiatry. 17, 748–758.
Laxer, K.D., Trinka, E., Hirsch, L.J., Cendes, F., Langfitt, J., Delanty, N., Resnick, T., Benbadis, S.R., 2014. The consequences of refractory epilepsy and its treatment. Epilepsy Behav. 37, 59–70.
Lévesque, M., Chen, L.-Y., Etter, G., Shiri, Z., Wang, S., Williams, S., Avoli, M., 2019. Paradoxical effects of optogenetic stimulation in mesial temporal lobe epilepsy. Ann. Neurol. 86, 714–728.
Löscher, W., Brandt, C., 2010. Prevention or modification of epileptogenesis after brain insults: experimental approaches and translational research. Pharmacol. Rev. 62, 668–700.
Mazzuferi, M., Kumar, G., Rospo, C., Kaminski, R.M., 2012. Rapid epileptogenesis in the mouse pilocarpine model: video-EEG, pharmacokinetic and histopathological characterization. Exp. Neurol. 238, 156–167.
Pitkänen, A., Lukasiuk, K., 2011. Mechanisms of epileptogenesis and potential treatment targets. Lancet Neurol. 10, 173–186.
Pitsch, J., Becker, A.J., Schoch, S., Müller, J.A., de Curtis, M., Gnatkovsky, V., 2017. Circadian clustering of spontaneous epileptic seizures emerges after pilocarpine-induced status epilepticus. Epilepsia 58, 1159–1171.
Salami, P., Lévesque, M., Benini, R., Behr, C., Gotman, J., Avoli, M., 2014. Dynamics of interictal spikes and high-frequency oscillations during epileptogenesis in temporal lobe epilepsy. Neurobiol. Dis. 67C, 97–106.
Salanova, V., Markand, O.N., Worth, R., 1994. Clinical characteristics and predictive factors in 98 patients with complex partial seizures treated with temporal resection. Arch. Neurol. 51, 1008–1013.
Spencer, S.S., Spencer, D.D., 1994. Entorhinal-Hippocampal interactions in medial temporal lobe epilepsy. Epilepsia 35, 721–727.
Staba, R.J., Wilson, C.L., Bragin, A., Jhung, D., Fried, I., Engel, J., 2004. High-frequency oscillations recorded in human medial temporal lobe during sleep. Ann. Neurol. 56, 108–115.
Wang, S., Lévesque, M., Avoli, M., 2019. Transition from status epilepticus to interictal spiking in a rodent model of mesial temporal epilepsy. Epilepsy Res. 152, 73–76.
Wieser, H.G., 2004. ILAE Commission Report. Mesial temporal lobe epilepsy with hippocampal sclerosis. Epilepsia 45, 695–714.
wen Xu, S., hui Xi, J., Lin, C., yang Wang, X., yuan Fu, L., Kralik, S.F., qian Chen, Z., 2018. Cognitive decline and white matter changes in mesial temporal lobe epilepsy. Med. U. S. 97.
Ylinen, A., Bragin, A., Nadasdy, Z., Jando, G., Szabo, I., Sik, A., Buzsaki, G., 1995. Sharp wave-associated high-frequency oscillation (200 Hz) in the intact hippocampus: network and intracellular mechanisms. J. Neurosci. 15, 30–46.
Zemlyanaya, A.A., Kalinin, V.V., Zheleznova, E.V., Sokolova, L.V., 2018. Dynamics of cognitive decline in patients with epilepsy during the course of disease (using executive functions as an example). Neurosci. Behav. Physiol. 48, 83–89.